



Experimental Study on Prestressed Concrete Beam-Column Joints which have Column-to-Beam Strength Ratios near 1

F. Kusuhara⁽¹⁾, H. Shiohara⁽²⁾

⁽¹⁾ Assistant Professor, The University of Tokyo, kusuhara@arch.t.u-tokyo.ac.jp

⁽²⁾ Professor, The University of Tokyo, shiohara@arch.t.u-tokyo.ac.jp

Abstract

For beam-column joints of reinforced concrete in moment resisting frames, a new type of failure is recently identified, which is called joint hinging mechanism. In the joint hinging failure mechanism, a beam-column joint reaches its maximum strength after tensile yielding of longitudinal bars passing through the joint for both horizontal and vertical direction. The joint hinging failure occurs typically in beam-column joints with low column-to-beam flexural strength ratios near one, regardless of the joint shear margin. The joint hinging mechanism causes lower strength mechanism and lower energy dissipation compared to beam hinging mechanism.

Meanwhile, beam-column joints of prestressed concrete are usually designed according to provisions with joint shear equations to prevent the joint failure before yielding of reinforcing bars or tendons. However, there is no guarantees that the joint hinging mechanism never occurs in beam-column joints of prestressed concrete. Hence, an experimental program on seismic performance of prestressed concrete beam-column joints with low column-to-beam flexural strength ratio was carried out.

This paper reports the test results. The test series consists of six specimens of one third scale. For four of the specimens, geometries and bar arrangements of beams and columns are identically and column-to-beam flexural strength ratios are one. These four specimens include one prestressed concrete beam-column joint without non-prestressed reinforcement, two prestressed reinforced concrete joints and one prestressed concrete without grout of tendons. In addition to them, two specimens in which column-to-beam strength ratio were 1.4 were loaded.

The test results show that: 1) joint hinging mechanism is occurred in beam-column joints which have column-to-beam strength ratios equal to one even for prestressed concrete and maximum story shear in cases of joint hinging mechanism are lower than cases of beam hinging mechanism, 2) larger column-to-beam strength ratio improves moment capacities of beam-column joints and leads beam hinging mechanism, 3) effects of location of tendons on strength are slight, 4) bondless between tendons and concrete reduce maximum strength of beam-column joints and 5) calculated moment capacities of prestressed concrete beam-column joints according to the theory for moment capacities of reinforced concrete beam-column joints in which dealt with prestress on beams and columns as axial forces agree with the test results.

Keywords: prestressed concrete; beam-column joint; joint hinging; ultimate strength; hysteresis loop



1. Introduction

For beam-column joints of reinforced concrete (RC) in moment resisting frames, a new type of failure is recently identified by one of the authors [1], which is called joint hinging mechanism. In the joint hinging failure mechanism, a beam-column joint reaches its maximum strength after tensile yielding of longitudinal bars passing through the joint for both horizontal and vertical direction. The joint hinging failure occurs typically in beam-column joints with low column-to-beam flexural strength ratios near one, regardless of the joint shear margin. The joint hinging mechanism causes lower strength mechanism and lower energy dissipation compared to beam hinging mechanism.

Meanwhile, beam-column joints of prestressed concrete (PC) are usually designed according to provisions with joint shear equations to prevent the joint failure before yielding of reinforcing bars or PC tendons. However, there is no guarantees that the joint hinging mechanism never occurs in beam-column joints of prestressed concrete. Hence, an experimental program on seismic performance of PC beam-column joints with low column-to-beam flexural strength ratio was carried out.

2. Test Program

2.1 Specimens

The test series consists of six specimens of one third scale beam-column sub-assemblages of crucial form. The test parameters are (1) with or without non-prestressed reinforcement (prestressed concrete (PC) or prestressed reinforced concrete (PRC)), (2) column-to-beam flexural strength ratio, (3) bond between tendons and concrete (with or without grout mortar), (4) location of PC tendons and (5) prestressing in columns. Figure 1 is a correlation diagram among specimens and Table 1 lists the specimens and their properties. The geometries and bar arrangement are shown in Fig. 2.

The columns and the beams have square sections and the depth and the width are 240 mm for all specimens. The columns and the beams of specimens No.1, No.3, No.5 and No.6 are PRC, while those of specimen No.2 are PC, without non-prestressed reinforcing bars, and the columns of specimen No.4 are RC without prestressing. The cross section and bar arrangement of the beams for specimens No.1, No.3 and No.4 are identically. The cross section and arrangement of PC tendons and non-prestressed reinforcement of specimen No.6 are same as specimen No.1, but with or without grout mortar is different. The sum of cross sectional area of PC tendons in specimen No.5 is equal to that of specimen No.1 but the PC tendons are located at the center of the section.

For four of the specimens including specimens No.1, No.2, No.5 and No.6, geometries and bar arrangements of beams and columns are respectively identical and column-to-beam flexural strength ratios are equal to one. As mentioned above, these four specimens include one prestressed concrete beam-column joint without non-prestressed reinforcement, two prestressed reinforced concrete joints and one prestressed concrete without grout of tendons. In addition to them, column-to-beam strength ratio for specimen No.3 and No.4 are 1.48 and 1.41 respectively. A contribution ratio of PC tendons to ultimate flexural capacity of a PRC section, called the prestressing ratio hereafter, ranged from 0.76 to 0.79.

PC tendons which passed through beams or columns were contained within a sheath tube and post tensioned up to the desired level of approximately 0.80 times the nominal yield strength of the tendon, i.e. 1020 MPa, after the concrete gained sufficient strength. After that, grout mortar was injected into the sheath tube except for specimen No.6.

The average compressive strength of the concrete by cylinder test was 54.6 MPa for specimen No.1 to No.4 and 63.3 MPa for specimen No.5 and No.6 respectively. The SBPD1275 steel was used for PC tendons. The yield strength of PC tendons ranged from 1406 MPa to 1449 MPa and rupture strain of them ranged from 8.1% to 10.5%. Mechanical properties of concrete, grout mortar and steel are listed in Table 2 and 3 respectively.

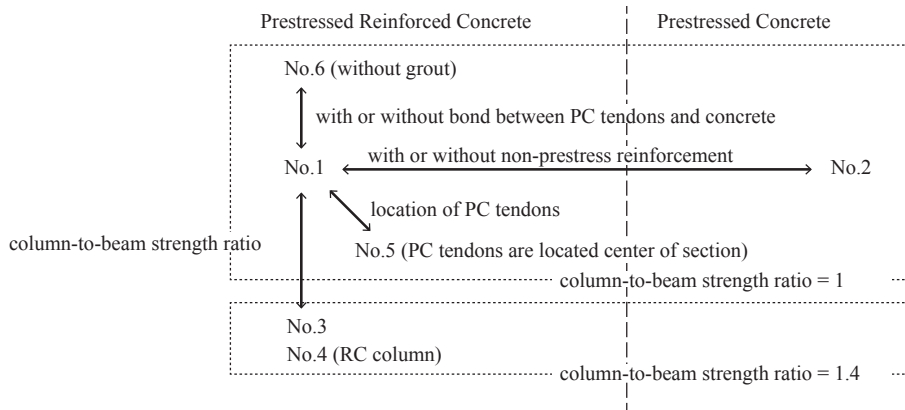


Figure 1 – Specimen correlation diagram

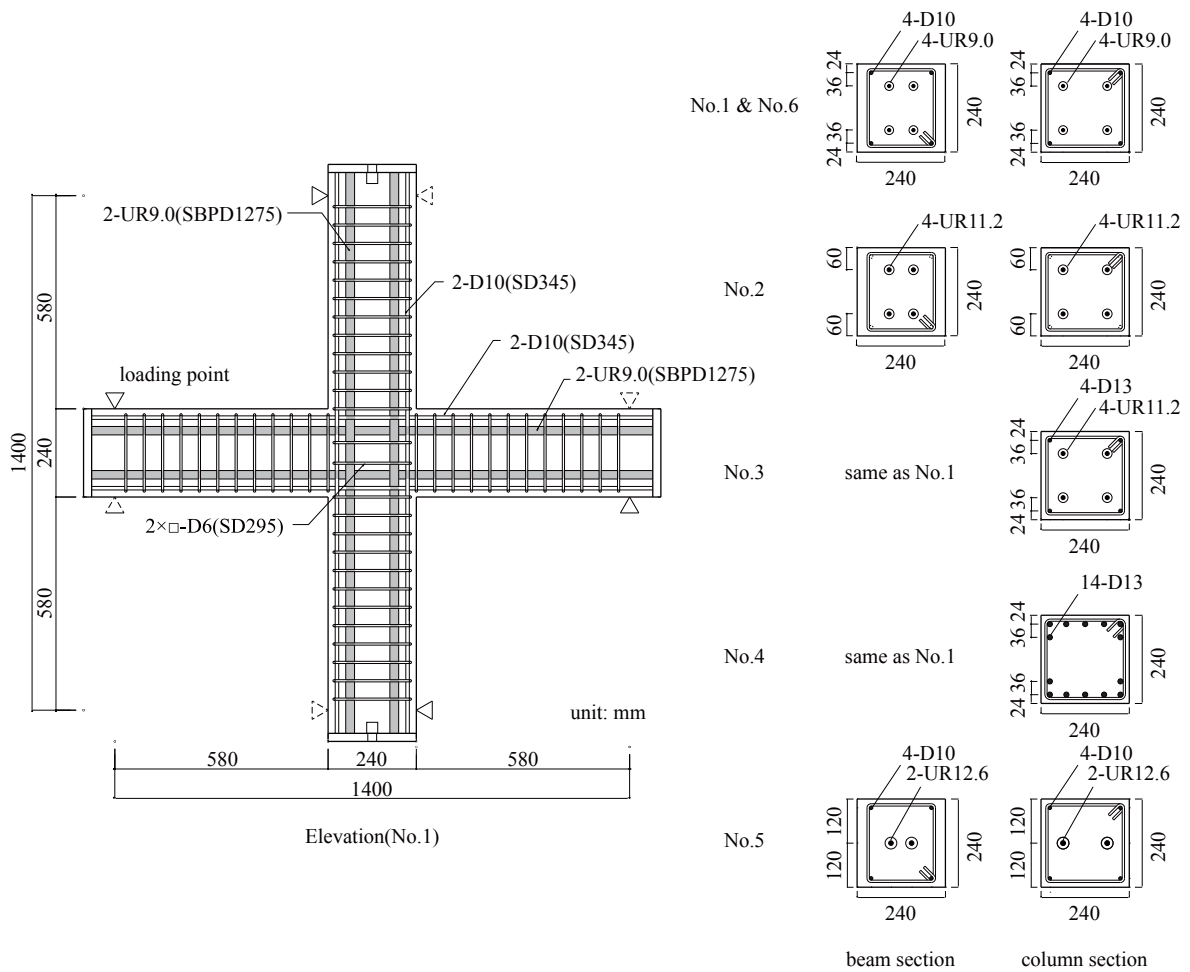


Figure 2 – Geometry and reinforcing details of specimens



Table 1 – Properties of specimens

Specimen		No.1	No.2	No.3	No.4	No.5	No.6
Beams	Type	PRC	PC	PRC	PRC	PRC	PRC
	Span	1400 (mm)					
	Section	240x240 (mm)					
	PC tendons	4-UR9.0	4-UR11.2	4-UR9.0	4-UR9.0	2-UR12.6	4-UR9.0
	Non-prestressed reinforcement	4-D10	N/A	4-D10	4-D10	4-D10	4-D10
	Prestressing ratio	0.79	1.0	0.79	0.79	0.77	0.78
Columns	Type	PRC	PC	PRC	RC	PRC	PRC
	Span	1400 (mm)					
	Section	240x240 (mm)					
	PC tendons	4-UR9.0	4-UR11.2	4-UR11.2	N/A	2-UR12.6	4-UR9.0
	Non-prestressed reinforcement	4-D10	N/A	4-D13	14-D10	4-D10	4-D10
	Prestressing ratio	0.79	1.0	0.76	0.0	0.77	0.78
Joint	Joint hoops	2 sets of D6 hoops					
Bond between PC tendons and concrete		bond					unbond
Column-to-beam strength ratio		1.0	1.0	1.0	1.48	1.41	1.0

Table 2 – Mechanical properties of concrete and grout mortar

	Specimen	Compressing strength (MPa)	Young's modulus (GPa)	Tensile strength (MPa)
Concrete	No.1 - No.4	54.6	35.7	4.03
	No.5 and No.6	63.3	32.4	3.31
Grout mortar	No.1 - No.4	68.0	45.0	
	No.5 and No.6	64.5	45.0	

Table 3 – Mechanical properties of PC tendon and steel

		Sectional area (mm ²)	Yield strength (MPa)	Young's modulus (GPa)	Tensile strength (MPa)	Rapture strain (%)
D6(SD295A)		32	334	186	479	23.6
D10(SD345)		71	389	188	532	17.6
D13(SD345)		127	380	197	547	20.5
UR9.0(SBPD1275)	No. 1, 3, 4	64	1425	221	1490	9.35
	No. 6		1449	229	1513	8.14
UR11.2(SBPD1275)		100	1406	234	1474	9.14
UR12.6(SBPD1275)		125	1430	224	1473	10.5

2.2 Test Setup and Loading Sequence

Figure 3 shows the loading setup and the instrumentation of story drift. A specimen is connected to the steel loading frame with PC rods. Both of the distances between two loading points for beams and columns are 1400 mm.

The upper horizontal loading beam is supported with two vertical loading columns with pinned joint at the both ends. The vertical loading columns are connected to a lower horizontal loading beam with pinned joints. The lower loading beam is fixed to a reaction floor. Four couples of fixtures are bound to the assumed counter-flexure point of the members of the beam-column joint specimen by PC rods. To connect the specimen to the loading frame, horizontal and vertical PC rods with diameters of 26 mm are connected from the frame to the fixtures at the loading points on the specimen. Spherical washers inserted between the nuts and the fixtures make the both ends of the PC rods pinned connections. Load cells are also inserted at one ends of vertical PC rods to measure the tensile force in the PC rods.

The lateral load was applied with a horizontal oil jack to an end of the upper loading beam. Since the stiff PC rods keep the distances of the loading points on the specimen from the loading frame constant, the deflection imposed on the loading frame is transferred proportionally to the specimen. The story shear is calculated from the tensile forces in the PC rods measured by the load cells installed at the end of vertical PC rods.

Statically reversed cyclic load with increasing amplitude was applied to simulate earthquake load. The loading history is shown in Fig. 4. The first cycle is load controlled before cracking. Then reversals with displacement control were applied up to story drift angle of 5.0%. No axial force is applied to the column.

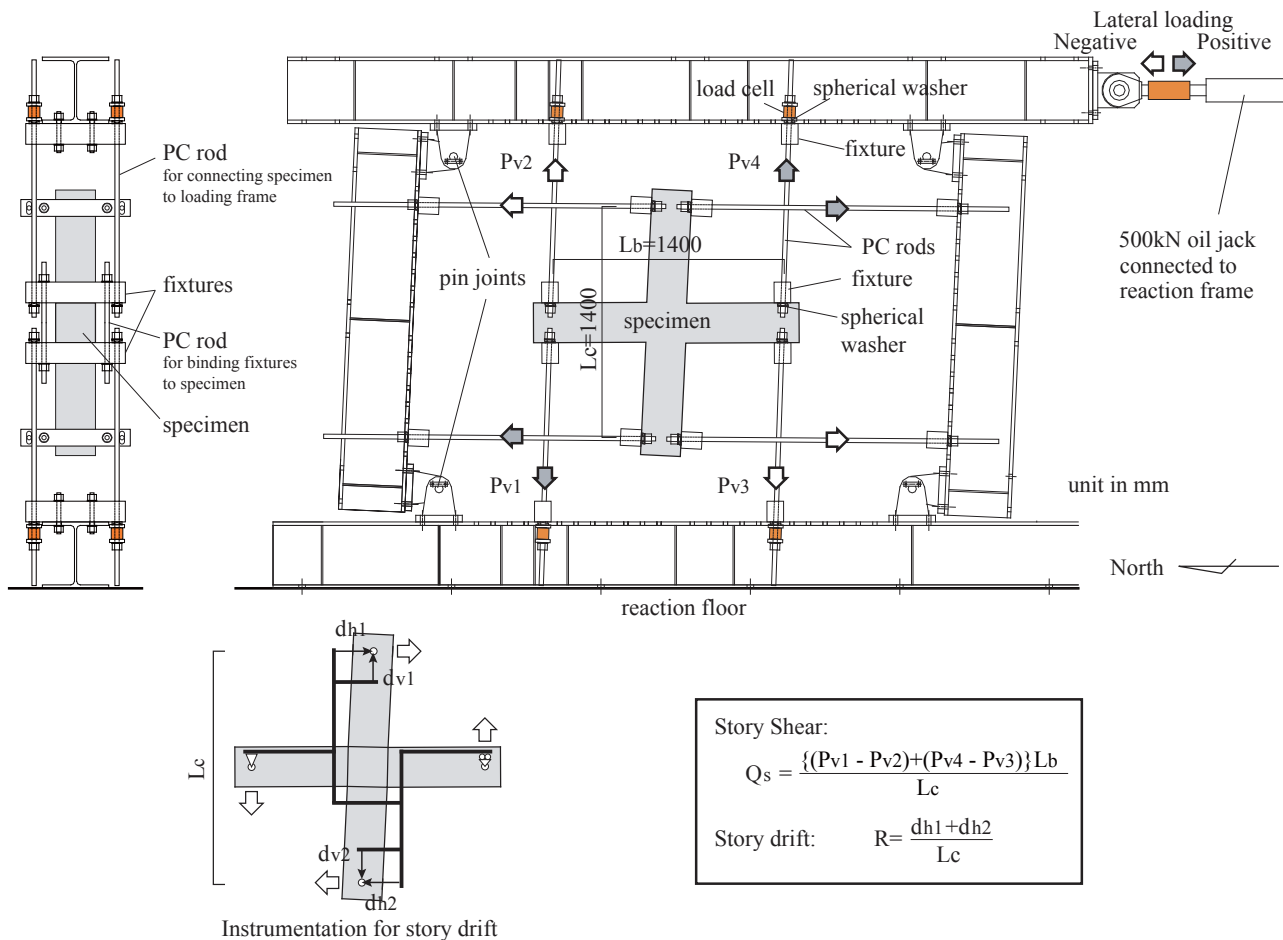


Figure 3 – Loading set up and instrumentation for story drift

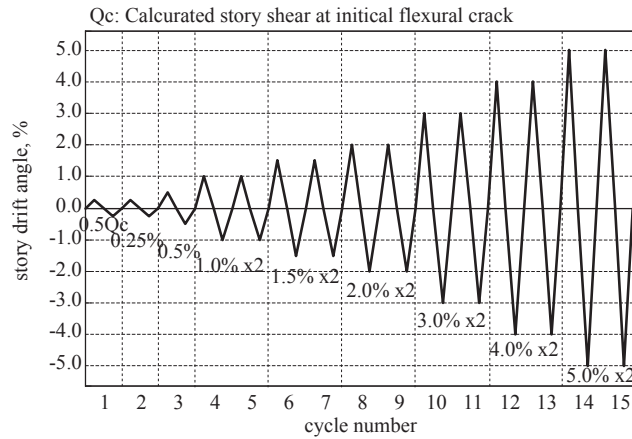


Figure 4 – Loading pattern

3. Test Results and Discussions

3.1 Overall behaviors

Photo 1 shows the failure pattern observed at the end of the cycles with story drift ratio of 3.0%. In all the specimens, diagonal cracking at two corners of the joint panels were observed at the load cycle of 0.25% story drift ratio. Then diagonal cracking at the center of joints were observed at the same load cycle.

At the load cycles with story drift ratio of 2.0%, concrete crush at the center of the joint initiated and cover concrete spalled off at the load cycle with story drift ratio of 3.0% or more in specimen No.1 and No.2, for which the column-to-beam strength ratio is equal to one. For specimen No.5, in which the PC tendons are located at the center of the sections, cracking pattern was similar to specimen No.1.

For specimen No.3 and No.4, for which the column-to-beam strength ratio is approximately 1.4, cracking and damage on concrete of the beam-column joint were minor.

After the load cycles with story drift ratio of 3.0%, opening of cracks at the ends of beams were dominant in specimen No.2, No.3 and No.4. Rupture of PC tendons in the beams was occurred at the load cycles with story drift ratio of 3.0 in specimen No.3 and No.4 and at the load cycles with story drift ratio of 4.0 in specimen No.2 respectively.

In specimen No.6, which has unbonded PC tendons, the cracks at both the corner and the center of the joint panel developed. And then crushing and spalling off of concrete at the center of the joint panel and the end of beams and columns were observed after the load cycles with story drift ratio of 3.0%.

Failure modes were joint hinging mechanism for specimen No.1, No.2, No.5 and No.6, while flexural failure of beams for specimen No.3 and No.4.

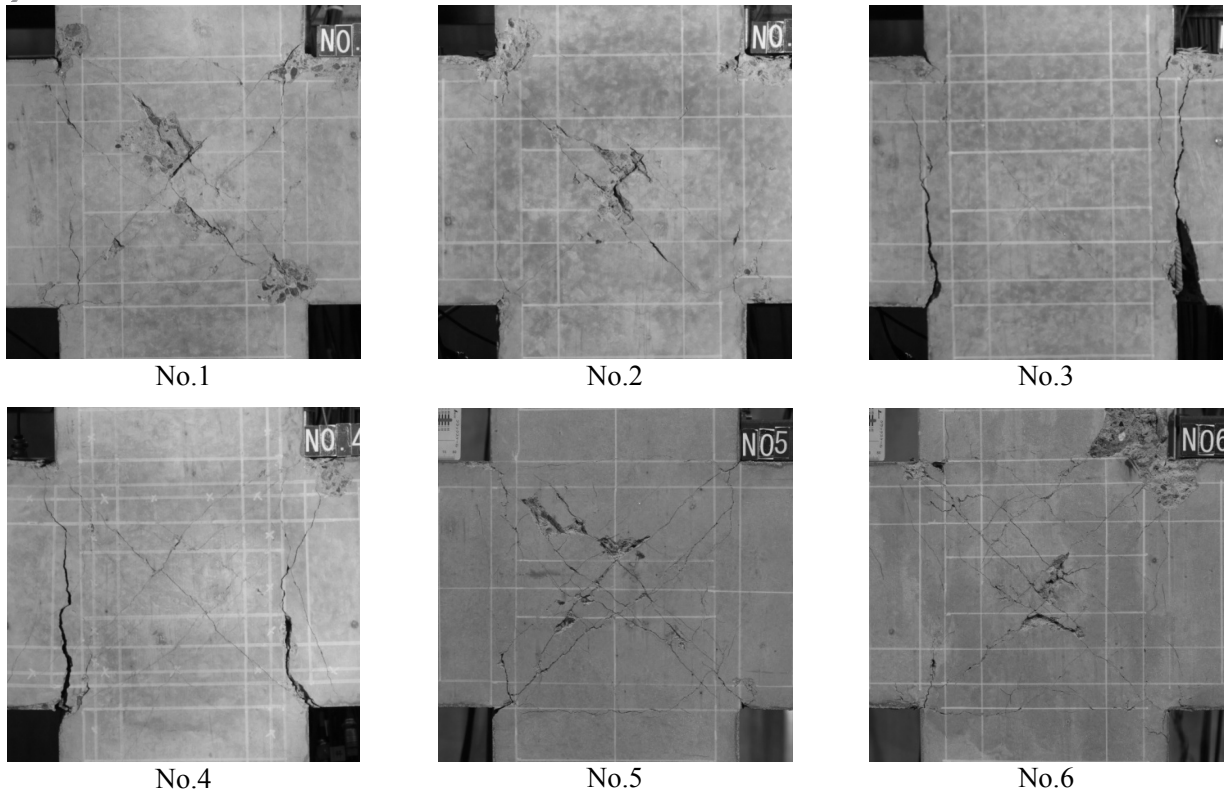


Photo 1 – Failure pattern of specimens at the end of load cycle of 3% story drift ratio

3.2 Story shear-story drift relationships

Figure 5 shows the story shear-story drift ratio relationships. Table 4 lists the observed strengths and deformations at major events including initial cracking, yielding of longitudinal steel, yielding of joint hoops and maximum story shear. Because of measurement failure for strain in PC tendons, the story shear and deformation at yielding of PC tendons were not obtained. The calculated story shear are compared in Figure 5. The calculated story shear is the story shear at the ultimate strength of beams. It was assumed that plane section remain plane in the deformation after the prestressing and mechanical properties of materials by tests were used in the calculation of ultimate flexural strength of the sections.

The maximum story shear of specimen No.1, No.2, No.5 and No.6, for which the column-to-beam strength ratio was equal to one, were attained at the load cycles with story drift ratio of 3.0%. The story drift ratio at the maximum story shear were smaller for specimen No.3 and No.4, for which the column-to-beam strength ratio is approximately 1.4. The maximum story shear of specimen No.1 is 4.7% smaller than that of specimen No.3 although the geometries and bar arrangement of beams in specimen No.1 and No.3 were identically. The maximum strength of specimen No.5 becomes 4.1% smaller than that of specimen No.1 by influence of location of PC tendons. In all specimens except specimen No.6, the attained maximum story shear exceeded the calculated story shear.

For specimen No.6, the maximum story shear decreased 13.5% from that of specimen No.1 by eliminating bond between PC tendons and concrete.

All PRC specimens except for specimen No.6 show first origin-oriented hysteresis loops, but then poor hysteresis curves with inverted-S-shape after the peak strength. The PC specimen named No.2 shows origin-oriented hysteresis loops throughout the test. Specimen No.6, in which the PC tendons are unbonded, shows spindle-shaped loops with large residual deformation at the unloading point after the loading cycles with story drift ratio of 2.0%. Strength degradation after the maximum strength is larger in specimen No.6.

Table 4 – Summary of Test Results

Specimen		No.1	No.2	No.3	No.4	No.5	No.6
Cracking at corner of joint	+	33.8 0.09	51.6 0.16	37.0 0.12	18.6 0.05	32.8 0.10	34.3 0.14
	-	-32.4 -0.06	-40.0 -0.08	-34.6 -0.09	-18.3 -0.02	-32.3 -0.09	-30.9 -0.11
Diagonal cracking at center of joint	+	52.9 0.23	70.2 0.29	60.1 0.29	38.8 0.19	45.9 0.19	48.9 0.25
	-	-48.0 -0.18	-67.5 -0.29	-51.6 -0.20	-36.2 -0.17	-44.4 -0.17	-47.2 -0.25
Yielding of non-prestressed reinforcement in beam at diagonal cracks in joint	+	77.1 0.75	/	81.0 0.72	74.6 0.78	71.7 0.70	71.3 1.10
	-	-70.0 -0.67	/	-68.3 -0.52	-70.5 -0.70	-63.2 -1.50	67.9 0.80
Yielding of non-prestressed reinforcement in column at diagonal cracks in joint	+	80.7 0.88	/	N/Y	95.5 1.76	73.3 0.75	-68.6 -0.86
	-	-72.0 -0.73	/	N/Y	-86.2 -1.73	-69.6 -0.71	-66.9 -0.81
Yielding of joint hoop		74.7 0.69	92.4 0.85	66.1 0.38	-67.0 -0.64	80.2 1.00	-63.4 -0.69
Attained maximum story shear	+	93.5 2.88	106.9 2.65	98.1 2.01	97.2 2.02	89.7 3.00	80.9 2.81
	-	-91.0 -3.01	-101.6 -1.98	-95.0 -2.02	-94.2 -2.01	-85.1 -2.00	-76.9 -2.00

upper row: story shear in kN, lower row: story drift angle in %, N/Y: no yielding

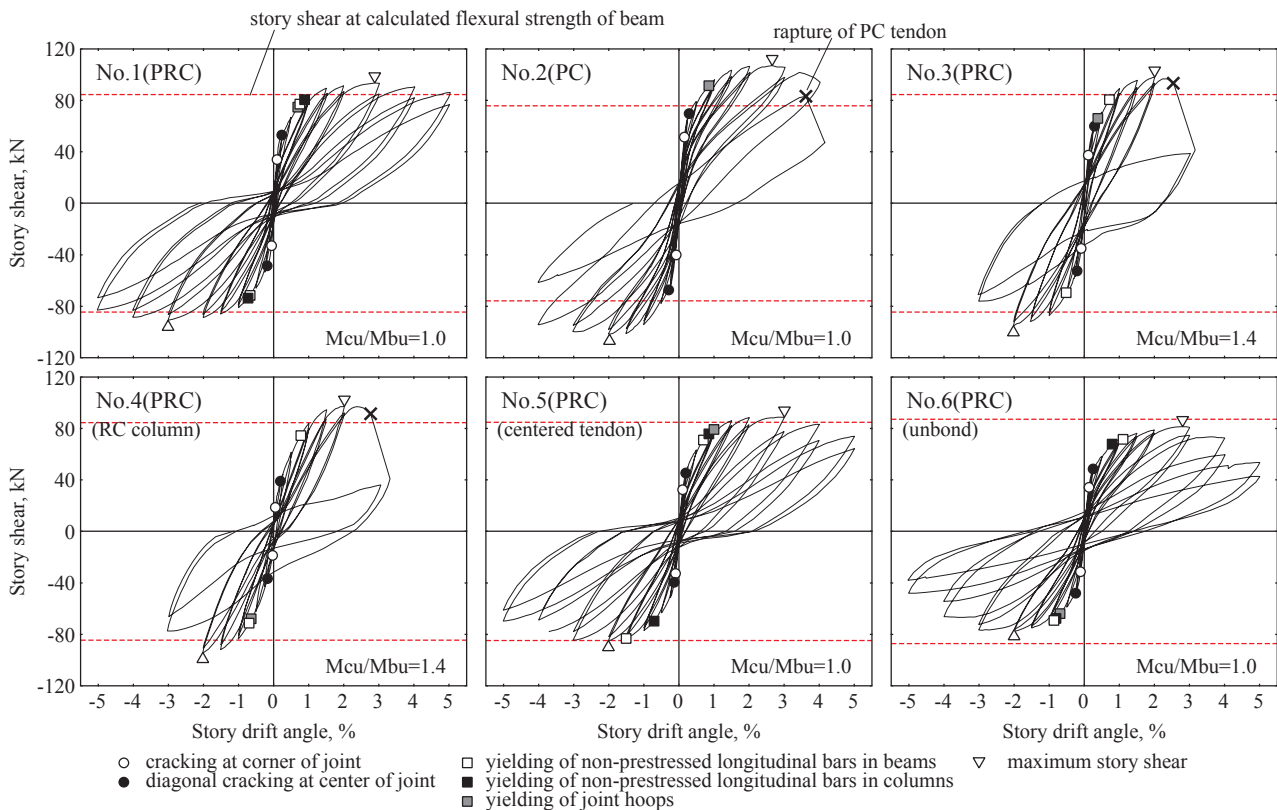


Figure 5 – Story shear - story drift relationships



3.3 Energy dissipation

Figure 6 shows the equivalent damping factor h_{eq} , which was calculated by Eq. (1), for each first and second loading cycle in the tests.

$$h_{eq} = \frac{1}{4\pi} \frac{\Delta W}{W_e} \quad (1)$$

where, ΔW : dissipated energy in each one loading cycle, W_e : potential energy at peak of loading cycle.

From the Comparison of specimen No.1 and No.3, large column-to-beam strength ratio increase energy dissipation. It may be the result that the failure mode changed by increasing column-to-beam strength ratio.

Figure 6 also indicates that the location of PC tendons in sections of beams and columns has no effect on energy dissipation of frames (from comparison of No.1 and No.5) and bondless between tendons and concrete makes equivalent damping factor large (from comparison of No.1 and No.6).

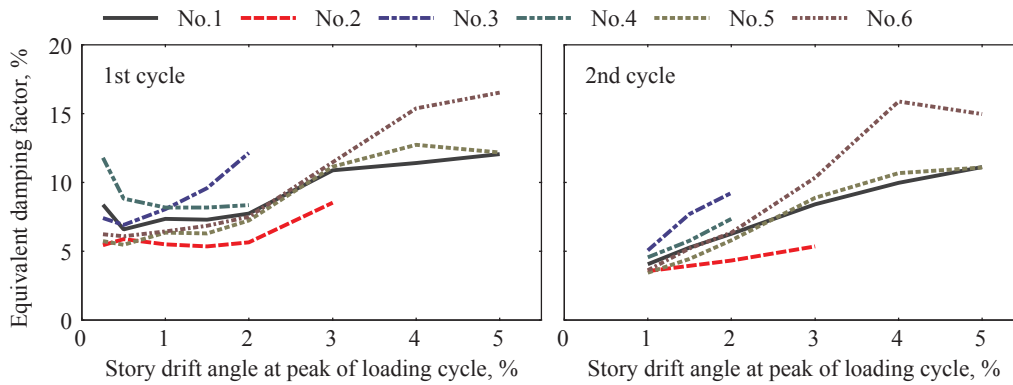


Figure 6 – Equivalent damping factor

3.4 Subcomponents of deformation

Figure 7 shows the subcomponents of story drift [2] observed in the tests. The story drift were divided into deformations due to the chord rotations of beams and columns, the rigid-body-rotations of beams and columns, the joint shear deformation and the rotations of triangular segments of beams-column joint panels.

In specimen No.1, No.5 and No.6, which formed joint hinging mechanism, the subcomponent due to joint deformations are increased after the story drift ratio of 3.0%, at which the maximum story shear were attained and crushing of concrete at the center of the joint panels started. In contrast, the rigid-body-rotations of beams and columns are dominant till the rapture of PC tendons in specimen No.3 and No.4.

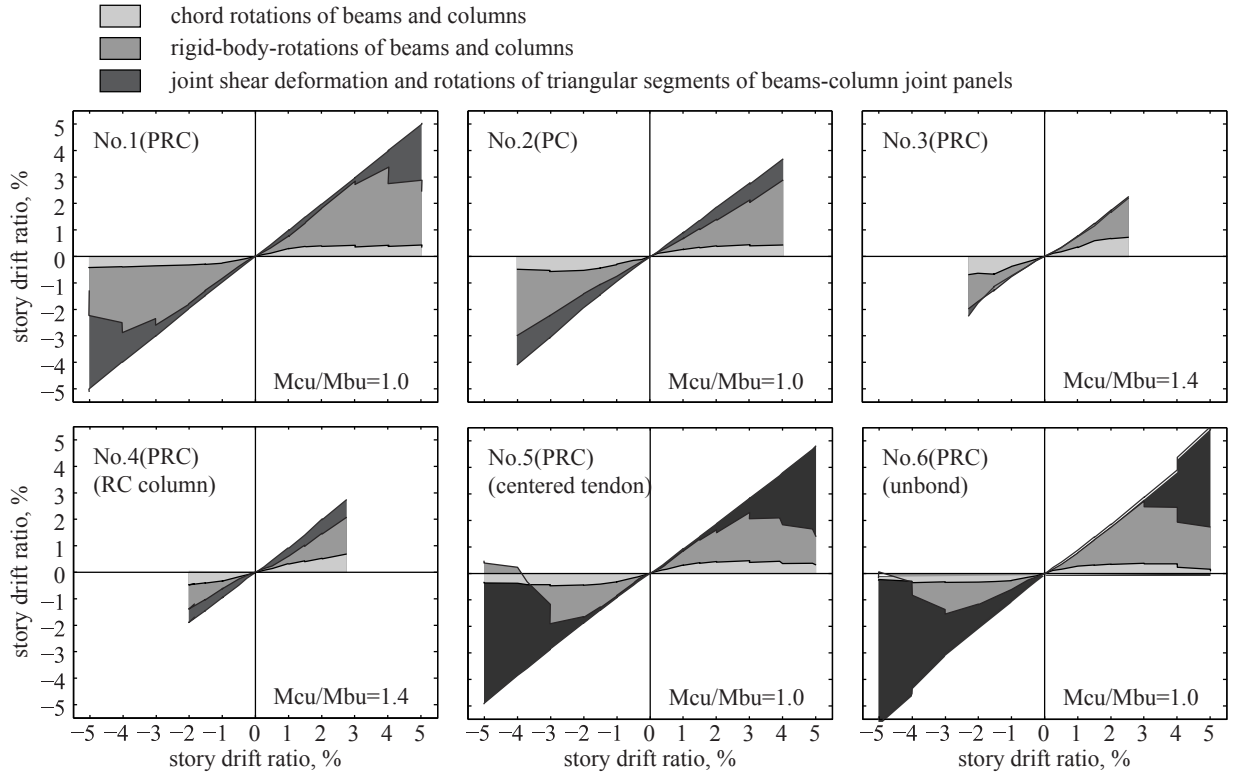


Figure 7 – Subcomponents of story drift

3.5 Predicted and observed story shear

Figure 8 compares calculated and observed maximum story shear. For ultimate strength of beam-column joints, the theory for ultimate strength of RC beam-column joints by the authors [3] was applied and the moment capacities of beam-column joints M_{ju} were calculated by Eq. (2). In the calculation, tension in PC tendons was treated as equivalent axial force in members of PC and PRC beam-column joints.

$$M_{ju} = \left[\frac{1}{2} (M_{jh} + M_{jv}) \right] / \left[1 - \frac{1}{2} \left(\gamma_h \frac{D_b}{H} + \gamma_v \frac{D_c}{L} \right) \right] \quad (2)$$

M_{jh} and γ_h are defined by Eqs. (3),

$$T_{by} = A_b f_y \geq \frac{1}{2} (1 - g_b) b_b D_b \beta_3 f_c - \frac{N_b + T_{hy}}{2} - \frac{V_c}{2}$$

$$M_{jh} = \left(g_b - \frac{T_{by} + (N_b + T_{hy})/2}{b_c D_b \beta_3 f_c} \right) \left(T_{by} + \frac{N_b + T_{hy}}{2} \right) D_b + \frac{1}{4} (1 - g_b)^2 b_b D_b^2 \beta_3 f_c \quad (3)$$

$$\gamma_h = g_b + 2 \frac{T_{by} + (N_b + T_{hy})/2}{b_c D_b \beta_3 f_c}$$



$$T_{by} = A_b f_y < \frac{1}{2}(1 - g_b) b_b D_b \beta_3 f_c - \frac{N_b + T_{hy}}{2} - \frac{V_c}{2}$$

$$M_{jh} = \left\{ 1 - \left(1 + \frac{b_c}{b_b} \right) \frac{T_{by} + (N_b + T_{hy})/2}{b_c D_b \beta_3 f_c} \right\} \left(T_{by} + \frac{N_b + T_{hy}}{2} \right) D_b$$

$$\gamma_h = 1 + 2 \left\{ \left(1 - \frac{b_c}{b_b} \right) \frac{T_{by} + (N_b + T_{hy})/2}{b_c D_b \beta_3 f_c} \right\}$$

while M_{jv} and γ_v are defined by Eqs. (4) as bellows.

$$T_{cy} = A_c f_y \geq \frac{1}{2}(1 - g_c) b_c D_c \beta_3 f_c - \frac{N_c + T_{my}}{2} - \frac{V_b}{2}$$

$$M_{jv} = \left(g_c - \frac{T_{cy} + (N_c + T_{my})/2}{b_c D_c \beta_3 f_c} \right) \left(T_{cy} + \frac{N_c + T_{my}}{2} \right) D_c + \frac{1}{4}(1 - g_c)^2 b_b D_c^2 \beta_3 f_c$$

$$\gamma_v = g_c + 2 \frac{T_{cy} + (N_c + T_{my})/2}{b_c D_c \beta_3 f_c} \quad (4)$$

$$T_{cy} = A_c f_y < \frac{1}{2}(1 - g_c) b_c D_c \beta_3 f_c - \frac{N_c + T_{my}}{2} - \frac{V_b}{2}$$

$$M_{jv} = \left\{ 1 - \left(1 + \frac{b_c}{b_b} \right) \frac{T_{cy} + (N_c + T_{my})/2}{b_c D_c \beta_3 f_c} \right\} \left(T_{cy} + \frac{N_c + T_{my}}{2} \right) D_c$$

$$\gamma_v = 1 + 2 \left\{ \left(1 - \frac{b_c}{b_b} \right) \frac{T_{cy} + (N_c + T_{my})/2}{b_c D_c \beta_3 f_c} \right\}$$

where, b_b, b_c : width of a beam and a column, D_b, D_c : depth of a beam and a column, g_b, g_c : distance ratio of longitudinal bars (ratio of distance between centroids of top and bottom non-prestressed bars to depth of a member), L, H : span length of a beam and a column (distance between loading points on beams or columns), T_{by}, T_{cy} : sum of yielding force of non-prestressed tensile reinforcements in a beam and a column ($T_{by}=A_b f_y, T_{cy}=A_c f_y$, where A_b, A_c : total sectional area of non-prestressed tensile longitudinal bars in a beam and a column and f_y : yield strength of non-prestressed bars), T_{hy} : sum of yielding force of joint hoops, T_{my} : sum of yielding force of intermediate longitudinal bars of a column, N_b, N_c : axial force in a beam and a column, f_c : compressive strength of concrete and β_3 : a factor to represent concrete stress of rectangular stress block ($\beta_3=0.85$ is assumed).

As mentioned above, the tensile force in PC tendons of a PC or PRC member is treated as resultant axial force in members. therefore,

$$N_b = N_{b0} + A_{bp} f_{py}$$

$$N_c = N_{c0} + A_{cp} f_{py} \quad (5)$$

where, N_{b0}, N_{c0} : axial force loaded on a beam and a column, A_{bp}, A_{cp} : total sectional area of tendons in a beam and a column and f_{py} : yielding strength of tendons.

Figure 8 indicates the calculation method for ultimate strength of beam-column joints can follow effects of design parameters including column-to-beam strength ratio, prestressing ratio and bond condition of PC tendons.

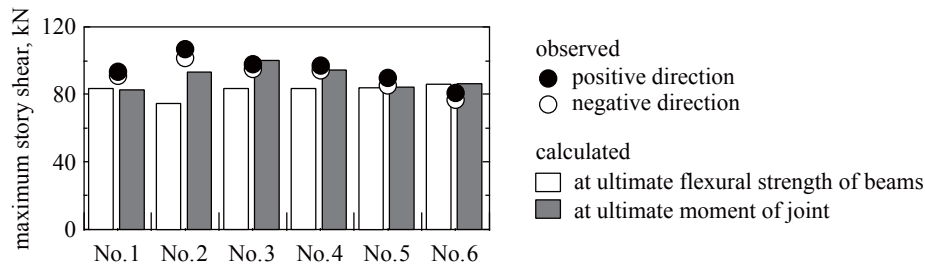


Figure 8 – Comparison of test and calculation for maximum story shear

4. Concluding Remarks

An experimental program on seismic performance of prestressed concrete beam-column joints which have column-to-beam flexural strength ratio near one was carried out in order to investigate joint hinging mechanism, which was recently identified for reinforced concrete beam-column joints, in prestressed concrete moment resisting frames. Concluding remarks drawn by this study are as follows.

- 1) Joint hinging mechanism developed in prestressed concrete beam-column joints which had column-to-beam strength ratios equal to one. Maximum story shear in cases of joint hinging mechanism did not reach the maximum story shear of the specimens in which beam hinging mechanism developed. This test result shows that low column-to-beam strength ratio near one causes joint hinging mechanism also for prestressed concrete joints.
- 2) Prestressed concrete beam-column joints which have column-to-beam strength ratios approximately 1.4 failed with beam hinging mechanism. It indicates that larger column-to-beam strength ratio improves moment capacities of beam-column joints and leads beam hinging mechanism.
- 3) Story shear-story drift relationship of the specimen in which the PC tendons were concentratedly located at the center of cross section of members was similar to that of the specimen in which the PC tendons were located on top and bottom layers. It means that effects of arrangement of tendons on strength of beam-column joints and energy dissipation of frames are slight if the location of centroids of PC tendons are not changed.
- 4) Maximum story shear of the specimen without grout mortar in sheath tube was smaller than that of the specimen with grout mortar. It means that bondless between tendons and concrete reduce maximum strength of beam-column joints.
- 5) Calculated moment capacities of prestressed concrete beam-column joints based on a theory for moment capacities of reinforced concrete beam-column joints agree with the test results. In the calculation, prestress in beams and columns shall be dealt as resultant axial forces in the members.

5. Acknowledgements

This work was supported by JSPS KAKENHI Grant Number JP24760445. The test was carried out with cooperation of Mr. K. Okihara and Mr. Y. Shu, who were graduate students of the University of Tokyo.

6. References

- [1] Shiohara H (2012): Reinforced Concrete Beam-Column Joints: An Overlooked Failure Mechanism, *ACI Struct. J.*, Vol. 109, No. 1, pp. 65–74.
- [2] Kusuhara F, Shiohara H (2006): New Instrumentation for Damage and Stress in Reinforced Concrete Beam-Column Joint, *Proc. of 8th U.S. National Conference on Earthquake Engineering*, San Francisco, USA.
- [3] Kusuhara F, Shiohara H (2014): Moment Capacity of Reinforced Concrete Interior Beam-Column Joints Based on a Theory of Flexural Resistance of Joints, *Proc. of 10th U.S. National Conference on Earthquake Engineering*, Anchorage, USA.